SPI instrumental background characteristics

P. Jean, G. Vedrenne, J.P. Roques, V. Schonfelder, B.J. Teegarden, A. von Kienlin, Jürgen Knödlseder, C. Wunderer, G.K. Skinner, G. Weidenspointner, et al.

A&A 411, L107–L112 (2003)
DOI: 10.1051/0004-6361:20031156

Astronomy & Astrophysics

SPI instrumental background characteristics⋆

P. Jean[1], G. Vedrenne[1], J. P. Roques[1], V. Schönfelder[2], B. J. Teegarden[3], A. von Kienlin[2], J. Knödlseder[1], C. Wunderer[2], G. K. Skinner[1], G. Weidenspointner[1,3,6], D. Attié[5], S. Boggs[4], P. Caraveo[8], B. Cordier[5], R. Diehl[2], M. Gros[5], P. Leleux[7], G. G. Lichti[2], E. Kalemci[4], J. Kiener[9], V. Lonjou[1], P. Mandrou[1], Ph. Paul[1], S. Schanne[5], and P. von Ballmoos[1]

[1] Centre d'Étude Spatiale des Rayonnements, CNRS/UPS, BP 4346, 31028 Toulouse Cedex 4, France
[2] Max Planck Institut fuer extraterrestrische Physik, Postfach 1312, 85741 Garching, Germany
[3] Laboratory for High Energy Astrophysics, NASA/Goddard Space Flight Center, Greenbelt, MD 20771, USA
[4] Space Science Laboratory, University of California Berkeley, CA 94720, USA
[5] DSM/DAPNIA/Service dAstrophysique, CEA Saclay, 91191 Gif-sur-Yvette, France
[6] Universities Space Research Association, 7501 Forbes Blvd. Seabrook, MD 20706-2253
[7] Institut de Physique Nucleaire, Universite catholique de Louvain, 1348 Louvain-la-Neuve, Belgium
[8] Istituto di Fisica Cosmica del CNR "G. Occhialini", via Bassini 15, 20133 Milan, Italy
[9] Centre de Spectrometrie Nucleaire et de Spectrometrie de Masse, IN2P3-CNRS, 91405 Orsay Campus, France

Received 15 July 2003 / Accepted 30 July 2003

Abstract. In its space environment the INTEGRAL observatory is subject to an intense irradiation by energetic cosmic-ray particles that leads, via nuclear interactions with the telescope and spacecraft materials, to an important background of false events. In this paper we present the characteristics of the instrumental background that is observed in the spectrometer SPI (SPectrometer of INTEGRAL). We explain the tuning that has been performed on the parameters of the anticoincidence system in order to optimise the telescope sensitivity over the full energy range. Temporal variations of the instrumental background are discussed and methods are proposed that allow for their modelling in first order.

Key words. gamma-ray: instruments

1. Introduction

The sensitivity of gamma-ray telescopes is limited by the instrumental background which comes mainly from the irradiation of the instrument by cosmic-ray particles. These particles directly or indirectly induce events in Ge detectors (GeDs) which disturb the observation of astrophysical signals. Several studies have been performed to understand, predict and reduce the instrumental background in germanium (Ge) spectrometers in space (Gehrels 1985; Dean et al. 1991; Gehrels 1992; Naya et al. 1996). Particular efforts have been made to estimate and minimize the instrumental background of SPI during its definition phase by performing extended background calculations for several spectrometer designs – e.g. mass distribution around the GeDs, shield thickness, passive material, characteristics of the detection system and background reduction techniques – (Jean et al. 1996a; Jean 1996b; Diallo et al. 1999).

Although the instrumental background can be understood in general terms as the response of the instrument to the incident (cosmic-ray, solar and trapped) particle flux and the natural radioactivity of local materials, the sources and the physical processes that induce this noise are multiple and complex. The main physical origin of the instrumental background can be presented/explained as follows. The impinging cosmic-ray protons create high energy secondary particles (p, n, π^0, π^+, γ...) in inelastic interactions with instrument nuclei. Resulting protons and neutrons can produce, by nuclear interactions in the materials, radioactive isotopes and isomers which decay with a delay[1] depending on their lifetimes, and then release β particles and/or de-excitation photons. When the β particles are emitted in the GeDs, they deposit their energies and generate a continuum energy distribution in the event spectrum. The de-excitation photons emitted by radioactive nuclei in passive material or in GeDs produce gamma-ray lines if they are totally absorbed in GeDs else they contribute to the continuum when they leave a fraction of their energy in GeDs via Compton scattering.

Send offprint requests to: P. Jean, e-mail: jean@cesr.fr

⋆ Based on observations with INTEGRAL, an ESA project with instruments and science data centre funded by ESA member states (especially the PI countries: Denmark, France, Germany, Italy, Switzerland, Spain), Czech Republic and Poland, and with the participation of Russia and the USA.

[1] Delay with respect to the instant of production of the unstable nucleus which is approximatively equal to the instant of interaction of the primary cosmic-ray proton.

The background events presented above originate from radioactive nuclei and we call them delayed components. However background events can also be induced very quickly after the interaction of primary cosmic-ray protons. Such events are called prompt background events. Some nuclei excited by secondary neutron-induced nuclear reactions de-excite promptly by electromagnetic transitions, also producing background gamma-ray lines. High energy secondary particles such as π^0, $\pi^{\pm}$ as well as primary cosmic-ray electrons trigger electromagnetic cascades that generate a continuum instrumental background spectrum. They also contribute to the 511 keV background line when they produce positrons by pair creation from secondary γ's and by the decay of π^+. Another prompt background component is the cosmic diffuse gamma-ray background which (1) enters through the SPI field of view and contributes mainly in the low energy range ($E \lesssim 100$ keV) and (2) passes through the shield without interacting with it.

The anticoincidence system (ACS) of SPI reduces significantly the rate of background events, as illustrated in Fig. 2. It allows the rejection of a significant fraction of prompt background events induced in hadronic and electromagnetic cascades. Indeed, these cascades consist generally of a large number of high-energy charged particles and photons which have a high probability of releasing energy in the active shield and thus triggering a veto signal. The ACS is less efficient in reducing the amount of delayed background components, moreover it is a source of secondary neutrons (see Leleux et al. 2003). Since the lifetimes of most of radioactive nuclei are much longer than the anticoincidence veto duration ($\sim\mu$s), the emitted particles (βs and γs) produce signals in GeDs that are not vetoed by the shield. Exceptions occur when (1) the radioactive nucleus decaying in passive material surrounding the GeD array or in a detector itself emits several photons (e.g. directly by nuclear de-excitation cascade or indirectly by annihilation of a β^+ particle), in this case one of the emitted photons can reach and trigger the ACS, rejecting the background event; (2) an isotope decays in the BGO shield and the released β particle and/or nuclear cascade photons triggers the ACS thus avoiding a possible background event in the GeDs.

This paper is structured as follows: in Sect. 2, the characteristics of the SPI background (rate, spectra by class of event, etc.) are described; Sect. 3 is dedicated to the analysis of the instrumental background variations as a function of the ACS parameters; in Sect. 4 temporal variations of the instrumental background are presented along with modelling methods; in the final section we compare the measured background spectrum with previous estimations. The origin and list of background gamma-ray lines are described in Weidenspointner et al. (2003) – see also Leleux et al. (2003).

2. Characteristics of the SPI background

Figure 1 shows the detector-averaged background spectrum of SPI for single GeD events (SE) and for pulse-shape discrimination event (PE), and double GeD events (ME2) involving two GeDs (see Diehl et al. 2003 for more details of event classes). In the case of multiple events the spectrum is built by summing the energies measured in adjacent GeDs. In both spectra one sees gamma-ray lines superimposed on a continuum. The levels of SE+PE and ME2 spectra are nearly equal above ~2 MeV. These spectra have been measured while the INTEGRAL observatory pointed towards an empty field during the commissioning phase. The ACS threshold was set at ~75 keV (75^{+50}_{-25} keV).

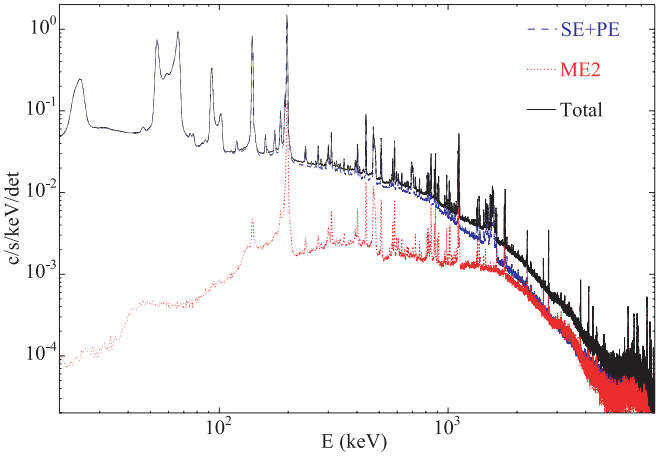

Fig. 1. Averaged SPI background spectrum. Single GeD event (SE+PE) and double detector event (ME2) spectra are presented separately. Peaks in the 1.4–2 MeV range of the SE+PE spectrum are electronic artifacts (Roques et al. 2003).

The total GeD rates are ~665 s^{-1} (35 s^{-1} $detector^{-1}$) and ~170 s^{-1} (9 s^{-1} $detector^{-1}$) in the 20 keV–8 MeV range for single and double detector events respectively. When normalized by GeD volume, the average spectrum of single detector events (SE+PE) of SPI is very similar to the measured spectrum of HIREGS, a BGO-shielded Ge spectrometer which flew on stratospheric long duration balloon flights over Antarctica (Boggs et al. 2002). At this high geomagnetic latitude, the cut-off rigidity is identical to that outside the magnetosphere.

The total 20 keV–8 MeV SE+PE rate does not show particular symmetric dependence on GeD position. This is not the case for specific rates in lines or continuum energy bands (some pictures are presented in `http://www.cesr.fr/~jean/integral.htm`). For instance, the 511 keV line rate is significantly higher for GeDs situated near the centre of the camera (GeDs 0 to 6) with respect to detectors on the periphery of the camera (GeDs 7 to 18). The maximum difference between the GeD rates in the 20 keV–8 MeV range is 5.6% (between GeD 8 and 12). However, it is only 2.9% (between GeD 5 and 8) when normalized to GeD mass (in s^{-1} g^{-1}) showing the effect of the Ge activation since more Ge mass implies more isotope yield and therefore more counts. The distribution of double-detector events shows an enhancement for GeDs facing IBIS. This may be due to a lower efficiency of the ACS block close to IBIS for rejecting background and/or to an increased background due to higher secondaries coming from the spacecraft and IBIS.

A comparison between two empty field observations shows that the relative total rate between single GeDs is quite stable – differences lower than 0.5% – while the total rate variation can be larger (see Sect. 4).

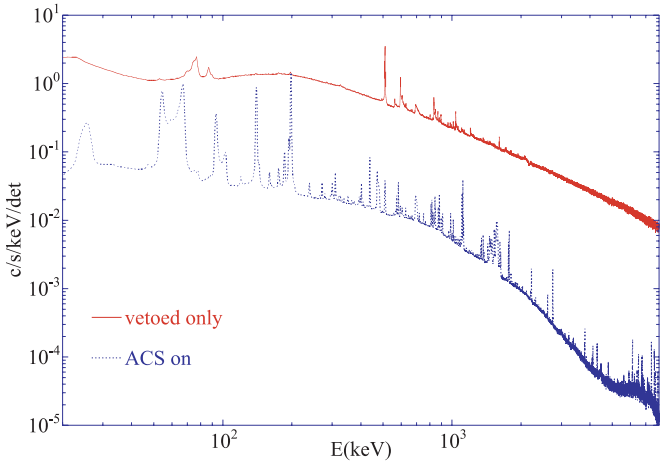

Fig. 2. SPI background spectra of GeD events in anticoincidence with an event in the ACS ("ACS on") and in coincidence with an event in the ACS ("vetoed only").

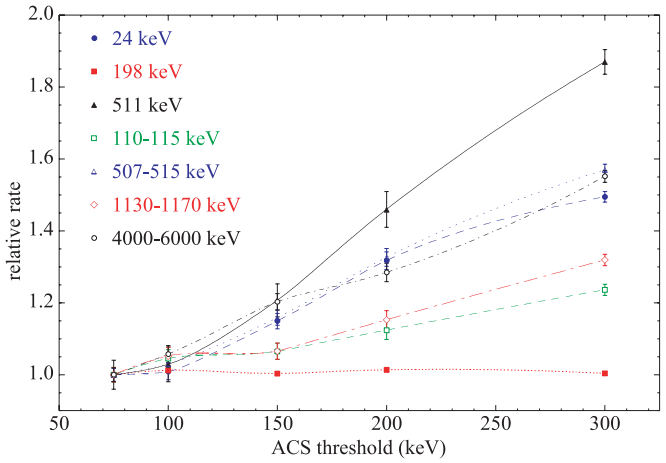

Fig. 3. Relative rate in lines (24 keV, 198 keV and 511 keV) and in continuum energy bands as a function of the ACS threshold.

3. Influence of the ACS parameters

The ACS significantly reduces the instrumental background as can be seen in Fig. 2, which shows background spectra of GeD events that did not coincide ("ACS on") or that did coincide ("vetoed only") with a trigger of the ACS (the latter ones are normally rejected onboard). The total rate in the 20 keV–8000 keV range changes by a factor ~25 between both configurations. The rate in the 511 keV line is increased by a factor ~130 when ACS is off. This demonstrates the high background suppression efficiency of the ACS for this line. The total rate is not significantly increased when the plastic scintillator is switched off. However the 511 keV background line rate increases by ~5%. This is less than expected by Jean et al. (1996a) due to the fact that at this epoch (1) the GeD capsules were planned to be in Be (the use of Al capsules increased the total background 511 keV line rate) and (2) the mass model used for this estimation was not complete (components not taken into account added other sources of 511 keV background).

Several measurements have been performed as a function of ACS configuration during the commissioning phase. Different threshold values and anticoincidence veto durations have been set and resulting background spectra analyzed. The goal of these tests was to find the optimal ACS configuration that maximizes the SPI sensitivity (i.e. reduces sufficiently the background rate without decreasing too much the livetime fraction). The following sections summarize the results of these tests.

3.1. ACS threshold

Figure 3 presents the variations of background line and continuum band rates for several ACS thresholds. The 511 keV line intensity increased by ~90% when the threshold changed from 75 keV to 300 keV, whereas the enhancement in continuum energy band rates was lower than 60%. The rate in the 198 keV line is shown because it is a tracer of the neutron flux irradiating the GeDs (see Naya et al. 1996). This line is due to the de-excitation of an isomeric state of the ^{71}Ge (with a half-life of 22 ms) which yields a 23 keV internal conversion electron and a 175 keV photon. The rate of the 198 keV line is independent of the ACS threshold since no secondary photons are emitted in the decay. As can be seen in Fig. 3, the variation of the neutron flux during these measurements is less than 1% so there is no variation of the activation between different settings. The 24 keV line rate, also plotted in Fig. 3, is due to both the same isomer (23 keV line) and an isomeric transition of the ^{58}Co at 25 keV. The latter line intensity is independent of the ACS threshold whereas the former changes since the 23 keV internal conversion electron is detected only if the 175 keV line escapes the GeD array without triggering the ACS. One would expect that the rate at 24 keV would be the lowest for threshold lower than 175 keV, increases suddenly at 175 keV and should not change above 175 keV. However the response of the ACS as a function of the energy is not a step function. Actually, the variation of the 24 keV line rate reflects the response of the ACS to 175 keV photons which escapes from GeDs, showing that the threshold is not sharp. The livetime decreased by 3% between the two tested extremum values of the ACS threshold. Consequently the variation of the sensitivity with respect to the ACS threshold is mostly due to the variation of the background rate. After this test, a threshold of ~75 keV was set.

3.2. ACS veto duration

Figure 4 shows the relative variation of the 511 keV line and 1150 keV continuum background rates as a function of the length of the veto window following ACS saturating events. The ACS non-saturating event veto duration was held at 750 ns (see Roques et al. 2003). An event in the ACS is tagged as saturating when the energy released is larger than ~150 MeV (150 ± 50 MeV). The livetime-corrected background rate increases with decreasing saturating event veto duration, showing an electronic shield-leakage effect and/or the effect of short-lifetime β^+ isotopes. An electronic shield-leakage effect appears when a BGO block has experienced a high energy deposit which triggers a saturating event. In this case,

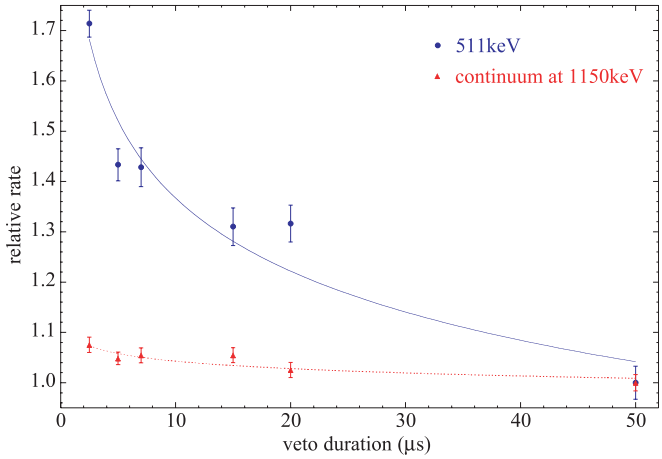

Fig. 4. Relative variation of the 511 keV line and continuum level at 1150 keV background rate as a function of the saturating event veto duration. The rates have been normalized to the values for the 50 μs veto duration. The lines are to guide the eye and have no quantitative meaning.

the charge-sensitive amplifier associated with this block delivers a signal that paralyses the electronics for an energy-dependent duration (called blocking time). Any events occurring in the block during the blocking time are not detected by the ACS. In order to reduce the blocking time effect, an additional electronic device allows the discharge of the charge sensitive amplifier. However it generates a voltage undershoot at the output of the charge sensitive amplifier with a duration which is a function of the energy released in the BGO block. This undershoot induces a variation of the shield threshold during this recovery time. The blocking time and recovery time effect can be reduced by increasing the veto duration for saturating events.

The 511 keV line rate increases by 70% between the extremum values of the saturating event veto durations whereas this variation is less than 10% for the continuum rate at ~1 MeV. One could think that the maximum value is the best one. However, the livetime fraction is 90% and 68% for veto durations of 2.5 μs and 50 μs respectively. Consequently the sensitivity is improved by less than ~10% at 511 keV when increasing the veto duration whilst it is damaged by ~10% at 1 MeV. After this test, a saturating event veto duration of 5.5 μs was set as optimal configuration.

4. Variations of the background

Thanks to the high-eccentricity orbit of the INTEGRAL observatory the impinging cosmic-ray proton flux which induces background is not modulated by the variation of cut-off rigidity and Earth-albedo gamma-ray and atmospheric neutron emissivities as it is for low Earth orbit observatories. As an example COMPTEL (on Compton-GRO) experienced background variations of a factor of ~4 (Kappadath et al. 1996). In the case of INTEGRAL, periodic and sporadic variations are observed but, excluding end of orbit (see Sect. 4.1) and solar flare events (see Sect. 4.2), the background rate variations are only a few percent. This temporal variation amplitude is however not always negligible because signals at the limit of sensitivity of the

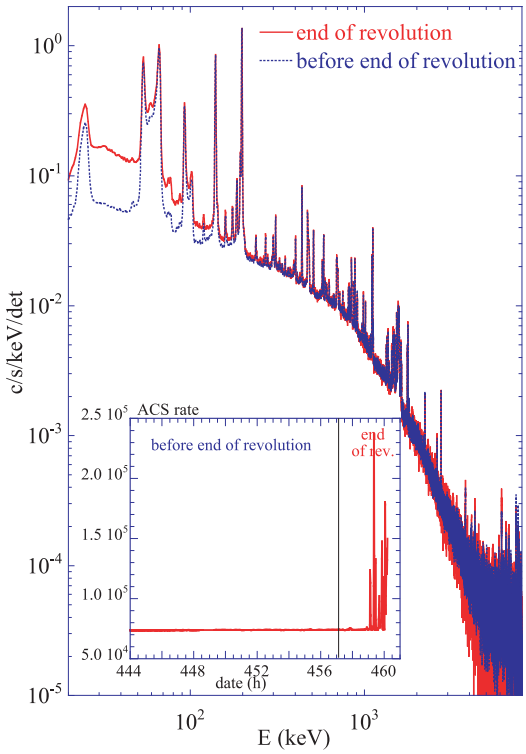

Fig. 5. Spectrum before and during the end of revolution. ACS rate as a function of time is also shown (inset).

instrument are often <1% of background level. In this section, the origins of the variation of the background are discussed and tracers for the background modelling are proposed to reduce its effects on the scientific analysis.

4.1. Periodic variations

Figure 5 shows background spectra recorded just before the end of a revolution when the spacecraft enters the outer electron belts. The ACS rate is also shown in the figure. A significant rate enhancement is visible at low energies. Observers should take care not to include in their analysis data obtained with abnormally high deadtimes recorded close to the end of a revolution.

The solar system magnetic field intensity is linked to active zones at the surface of the sun and varies with the solar rotation, inducing a quasi-periodic modulation (periods ~27 days) of the cosmic-ray flux at the level of the Earth orbit. This modulation, visible in the GeD rate (see Fig. 6) has an amplitude of ~10% and is also present in the ACS rate.

4.2. Solar flare

When the sun flares it ejects high-energy protons which can reach the spacecraft. Depending on the strengh of the flare, the flux of protons is more or less intense and their energy spectra are usually soft (proton energies <100 MeV). Consequently, solar flare protons do not produce a lot of secondary neutrons when they irradiate the observatory. Figure 7 shows spectra before and during the November 9th, 2002 solar flare. The GeD

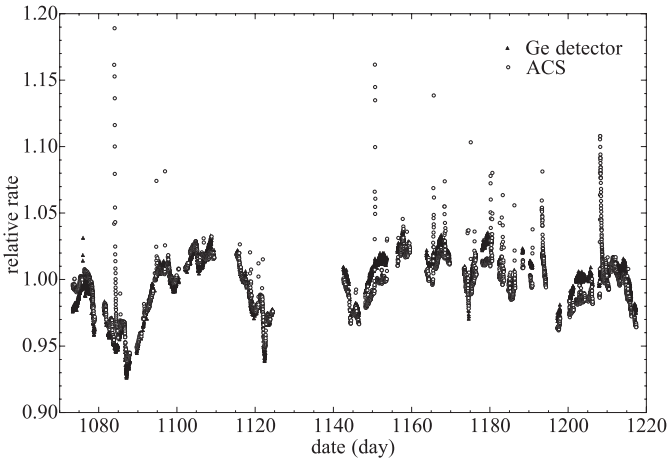

Fig. 6. Variation of the total GeD and ACS rates as a function of time. The large excesses in the ACS rate are due solar flares and electron belts entry. Dates are relative to 2000 January 01, 0h00.

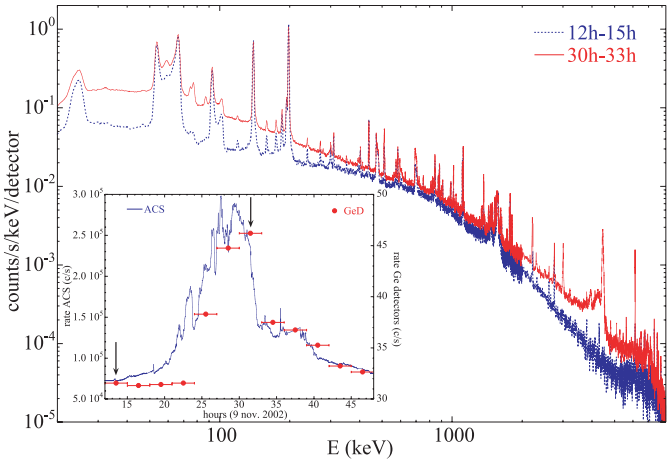

Fig. 7. Spectrum before and at the maximum GeD rate during the solar flare of november 9, 2002. ACS and GeD rates as a function of time are also shown (inset). Arrows show the dates where the spectra have been recorded.

rate has increased by ~50%. Continuum and some line rates show significant intensity enhancements. Lines which experienced strong enhancements in their intensities mostly come from local Al, C and O nuclei, while neutron-induced Ge lines except for prompt Ge(n, n′) lines slightly decreased during the flare. Prompt excitation of Al external to the shield by solar protons induced new lines above 2 MeV (e.g. at 2211 keV and 3004 keV). Observers should take care not to include in their analysis data obtained during irradiation of INTEGRAL by solar flare protons.

4.3. Long term variations

INTEGRAL was launched close to the end of a solar maximum activity period. A slow enhancement of the cosmic-ray intensity by ~50% is expected over the next 4 years i.e. until the solar minimum activity period is reached. Radioactive build-up will also induce a long-term enhancement in rates of lines emitted by long half-life isotopes. Examples are shown in Fig. 8

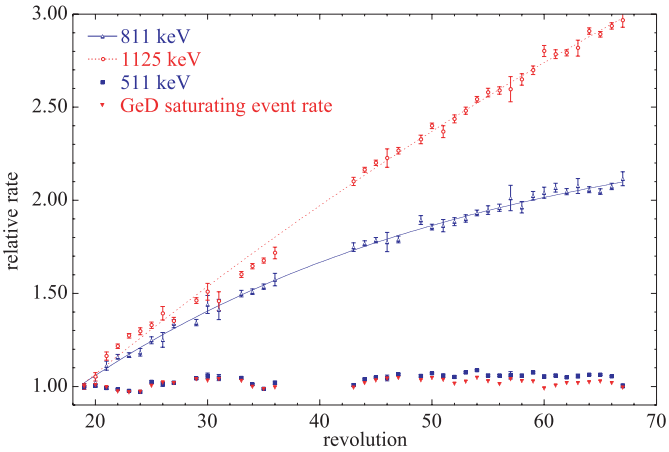

Fig. 8. Rate of the 811 keV (^{58}Co), 1125 keV (^{65}Zn), 511 keV (e^+e^-) and GeD saturating events as a function of revolution number. Rates are normalized with respect to the rates measured during revolution 19.

with the 811 keV and 1125 keV lines associated with the ^{58}Co ($T_{1/2}$ = 70.8 days) and the ^{65}Zn ($T_{1/2}$ = 244 days) respectively. The 511 keV line is also shown in Fig. 8. No enhancement is visible during the period discussed here; the line rate varies as the Ge saturating event rates except between revolution 49 and 66 when the observatory pointed toward the Galactic Center region.

4.4. Tracers of the background

ACS event and ACS- and GeD-saturating event rates vary with the solar-modulated cosmic-ray proton intensity. For particular scientific analyses, background models based on an empty field observation rescaled using these tracers can significantly reduce the effects of cosmic-ray proton intensity variations (see Fig. 8). We performed fits of models based on these tracers to the measured rate per pointing and per detector. The background model is proportional to the tracer with a constant of proportionality that is chosen to minimize the χ^2. The model can also be proportional to the products of tracer and the value $\langle r_d \rangle$ of the relative rates between detectors, since it is relatively stable (see Sect. 2). $\langle r_d \rangle$ is obtained from empty-field observations and is based on the rates averaged over all pointings. Figure 9 presents results of χ^2 tests of background models performed on continuum energy ranges and on lines. Models based on ACS (acs) event and ACS- (acssat) and GeD-saturating (gedsat) event rates generally improve significantly the reduced χ^2 with respect to the models which assume a constant in time background (named "$r_{p,d}$ = const." and "$r_{p,d}$ = const. $\langle r_d \rangle$" in Fig. 9). However, depending on the energy range or line, systematic differences are not completely removed partly due to the fact that long term variations such as radioactive build-up are not taken into account with these tracers.

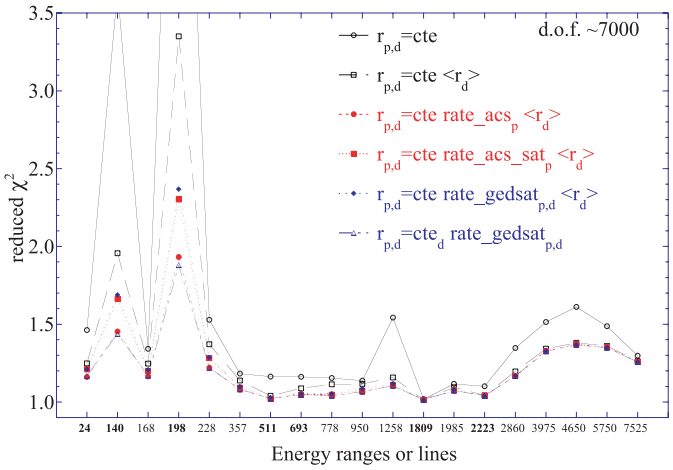

Fig. 9. The reduced χ^2 for the fit of background models to the measured rates as a function of the energy range. Models defined with $\langle r_d \rangle$ assume that the relative rate between GeDs is constant. Energy of background lines are written in bold.

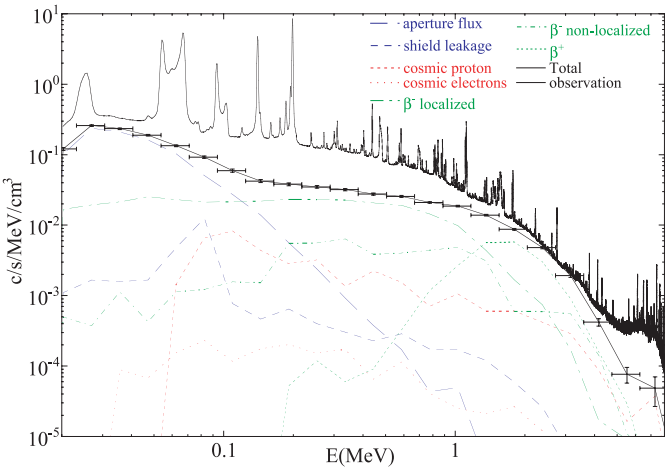

Fig. 10. Comparison of continuum background spectrum estimated by simulation before the launch of INTEGRAL with the measurements. Background components are shown separately.

5. Conclusions

Figure 10 presents a comparison of the continuum background spectrum calculated in March 2002 with the measurements. Important differences in the continuum component are visible in the 100–900 keV energy range as well as above 6 MeV, due to an underestimation of the β decay and neutron capture components and the fact the contribution of instrumental lines to the continuum (via Compton scattering) was known not to have been taken into account in the calculation. More recent calculations, including lines, have been performed and are presented in Weidenspointner et al. (2003).

The ACS parameters (threshold of ~75 keV and saturating event veto duration of 5.5 μs) have been tuned to optimize the sensitivity of SPI (Roques et al. 2003).

The total background variations are weak[2] (less than a few percent) thanks to the high eccentricity orbit and high perigee of the INTEGRAL observatory. Although there are temporal variations which can produce artifacts and/or introduce systematic errors in the scientific analysis, they can be estimated using tracers such as the ACS rate and the saturating GeD rate. Extensive studies and modelling of the continuum and line backgrounds are in progress in order to provide methods to improve the data analysis and reduce systematic errors.

Acknowledgements. The SPI project has been completed under the responsibility and leadership of CNES. We are grateful to ASI, CEA, CNES, DLR, ESA, INTA, NASA and OSTC for their support.

References

Boggs, S., Jean, P., Slassi-Sennou, S., et al. 2002, Nucl. Instr. and Meth., A 491, 390
Dean, A. J., Lei, F., & Knight, P. J. 1991, Space Sci. Rev., 57, 109
Diallo, N., Jean, P., Legrain, R., et al. 1999, Nucl. Instr. and Meth., A 455, 545
Diehl, R., Baby, N., Beckmann, V., et al. 2003, A&A, 411, L117
Gehrels, N. 1985, Nucl. Instr. and Meth. A, 239, 324
Gehrels, N. 1992, Nucl. Instr. and Meth. A, 313, 513
Jean, P., Naya. J., Ballmoos von P., et al. 1996a, SPIE, 2806, 457
Jean, P. 1996b, Ph.D. Thesis, Université Paul Sabatier
Kappadath, S. C., Ryan, J., Bennet, K., et al. 1996, A&A, 120, 619
Leleux, P. Albernhe, F., Borrel, V., et al. 2003, A&A, 411, L85
Naya, J. E., Jean, P., Bockholt J., et al. 1996, Nucl. Instr. and Meth. A, 368, 832
Roques, J. P., Schanne, S., von Kienlin A., et al. 2003, A&A, 411, L91
Weidenspointner, G., Gros, M., Kiener, J., et al. 2003, A&A, 411, L113

[2] Except during solar flare and in electron belts (shortly before end-of-orbit)